Journal of Saudi Chemical Society (2015) 19, 436–441

King Saud University

Journal of Saudi Chemical Society

www.ksu.edu.sa
www.sciencedirect.com

ORIGINAL ARTICLE

Assessing the quantum mechanical level of theory for prediction of UV/Visible absorption spectra of some aminoazobenzene dyes

Asif Mahmood [a,*], Salah Ud-Din Khan [b], Fazal ur Rehman [c]

[a] Department of Chemistry, University of Sargodha, Sargodha, Pakistan
[b] College of Engineering, PO Box 800, King Saud University, Riyadh 11421, Saudi Arabia
[c] Department of Mathematics and Statistics, University of Agriculture, Faisalabad, Pakistan

Received 4 May 2014; revised 3 June 2014; accepted 5 June 2014
Available online 16 June 2014

KEYWORDS

UV/Visible spectra;
Solvation models;
CAM-B3LYP;
LC-BLYP;
BHandHLYP;
PBE0

Abstract This quantum mechanical study was performed to assess the accuracy of level of theory for the prediction of UV/Visible spectra of aminoazobenzene dyes. Four solvation models (PCM, I-PCM, SCI-PCM and IEF-PCM) and four functionals (CAM-B3LYP, LC-BLYP, BHandHLYP and PBE0) were tested. Double and triple zeta basis sets with and without polarization and diffuse functions were used. All the solvation models showed the same level of error in the prediction of UV/Visible spectra. Among the tested functionals, PBE0 showed a close agreement to experimental values. Among, different basis sets, 6-311++G showed best results.

1. Introduction

At present, the use of computational tools is becoming an important part of fundamental investigation and studies with the purpose to simulate the UV/Vis spectra of organic compounds. In this context, the most commonly used methods are semi-empirical and density-functional theory (DFT). The semiempirical methods are fast and accurate to investigate those compounds, which are similar to systems for which the method was parameterized [1]. DFT offers the best compromise between accuracy and computational performance. In usual practice, the electronic spectra are calculated using time-dependent density-functional theory (TD-DFT) [2,3] and numerous successes of this technique have been recently reviewed [4]. The time-dependent density functional theory (TD-DFT) has been widely used by different authors for calculations of excitation energies and oscillator strengths for

Abbreviations: PCM, polarizable continuum model; I-PCM, implicit PCM; SCI-PCM, self-consistent isodensity PCM model; IEF-PCM, integral equation formalism PCM model; B3LYP, Becke three-parameter Lee-Yang-Parr exchange-correlation functional; CAM-B3LYP, Coulomb attenuated B3LYP functional; LC-BLYP, long-range corrected BLYP; BHandHLYP, Becke-Half-and-Half-LYP; PBE0, Perdew–Burke–Ernzerhof exchange-correlation functional; DMSO, dimethyl sulfoxide

* Corresponding author. Mobile: +92 333 8192709.
E-mail address: asifmahmood023@gmail.com (A. Mahmood).

Peer review under responsibility of King Saud University.

ELSEVIER Production and hosting by Elsevier

http://dx.doi.org/10.1016/j.jscs.2014.06.001

organic systems [5–16]. In a series of comparative studies, different functionals were used with the TD-DFT methodology [13–16]. In addition, the quantum chemical methods also emerged as an easy way to stimulate the UV/Vis spectra. Here, it is important to note that the UV/Vis spectra are strongly dependent on the theoretical approaches, with inclusion of electronic correlation and extended basis set being necessary to achieve satisfactory accuracy.

Quantum mechanical methodologies are also used to explore the theoretical chemistry behind reactive systems, to compare the relative chemical reactivity of different systems and, by extension, to predict the reactivity of new systems. Computational techniques have become very valuable tools in the study of the reactivity of compounds [17–20]. Calculations furnish information at a molecular level about the mechanistic features of the reaction and can contribute in controlling and improving the processes.

Schafer stated that, in the majority of cases, IR or Raman spectra can be accurately computed with the help of quantum mechanical methods that could be found in many computational chemistry packages [21]. However, it is not the case for UV/Vis spectra of large conjugated molecules.

The quantum chemistry literature contains a large number of functional and basis sets. The occasional user of ab initio programs probably wishes to ignore all but the two or three sets which, through habitual use, have become personal favorites. Unfortunately, this attitude has its drawbacks. Intelligent reading of the literature requires at least fundamental knowledge of the advantages and limitations of other functional and basis sets. Information concerning the likely accuracy of a specific functional or basis set for a particular property is essential in order to judge the adequacy of the computational method and, hence, the soundness of the results. Occasionally, for reasons of economy or computational feasibility, a basis set is selected for which the computed results are nearly without significance.

Aminoazobenzene dyes were selected for this study because experimental UV/Vis spectra in different solvents are available. These dyes also showed a remarkable change in different solvents. Azo dyes are one of the important classes of colorants [22]. The driving force behind this research work was to find theoretical methodology to stimulate the UV/Vis spectra with reasonable accuracy and computational cost. In this study TD-DFT methods with the CAM-B3LYP, LC-BLYP, BHandHLYP and PBE0 functionals using different basis sets, including polarization and diffuse functions, were used to compute the UV/Vis spectra. Solvent effect was undertaken using various solvation models (PCM, I-PCM, SCI-PCM and IEF-PCM).

2. Computational methodology

Density functional theory was used in all types of calculations [23–25]. The structures of dyes were optimized using B3LYP exchange–correlation functional and the 6-311(d,p) basis set implemented in Gaussian09 program [26]. The equilibrium geometries of the molecule were determined via the gradient technique. The ground-state geometry of each molecule has been fully optimized until the RMS residual force is smaller than 1×10^{-5} au (TIGHT threshold in Gaussian). The force constants and vibrational frequencies were determined by computing the analytical frequencies at the stationary points obtained after optimization to confirm that they were true minima.

UV/Visible spectra were simulated using PBE0 functional and 6-311(d,p) basis set in three solvents (cyclohexane, acetone and DMSO). PCM, SCI-PCM, I-PCM and IEF-PCM solvation model were used. All the solvation models showed almost similar results for three dyes in three solvents. To further study the effect of functional and basis sets, only one solvation model and one solvent were selected. This selection was made to reduce the computational cost. Four functionals (CAM-B3LYP, LC-B3LYP, BHandB3LYP and PBE0) were used.

To choose the best basis set, we tested Pople valence-multiple-f basis sets associated with polarization and diffuse functions. The tested basis sets can be grouped into three classes, i.e. (i) unpolarized Pople valence-double-f basis set (6-31G), (ii) Pople valence-double-f basis sets [6-31G(d,p),6-31 + G(d,p)and 6-31 + + G(d,p)], and (iii) Pople valence-triple-f basis sets [6-311G (d,p), 6-311 + G (d,p), and 6-311 + + G (d,p)].

3. Cluster analysis

Cluster analysis is a major technique for classifying a 'mountain' of information into manageable meaningful piles. It is a data reduction tool that creates subgroups that are more manageable than individual datum. It examines the full complement of inter-relationships between variables. Cluster analysis is concerned with classification. In cluster analysis there is no prior knowledge about which elements belong to which clusters. The grouping or clusters are defined through an analysis of the data. Subsequent multi-variate analyses can be performed on the clusters as groups. The clustering method uses the dissimilarities or distances between objects when forming the clusters. The statistical program calculates 'distances' between data points in terms of the specified variables. Objects within the clusters are similar whereas objects in different clusters are dissimilar. This exploratory method is used to discover the data structure not only among observations, but also among variables, arranged into a tree diagram, usually called a dendrogram. The clusters are linked at increasing levels of dissimilarity. In this study, the commonly applied average group and Ward's clustering methods were used. The Euclidean distance was used as a similarity measure.

4. Results and discussion

The accuracy of the calculated λ_{max} values was assessed against the values obtained experimentally. This study was performed to assess the performance of quantum chemical methods to stimulate the UV/Visible spectra of aminoazobenzene dyes. Structures of dyes are given in Fig. 1. These dyes were selected for this study because experimental UV/Visible data are available in different solvents and these dyes are small in size. Small structure is required for minimum computational cost.

4.1. Effect of solvation model

In the real world most of physico-chemical processes take place in solution and molecular properties exhibit a more or

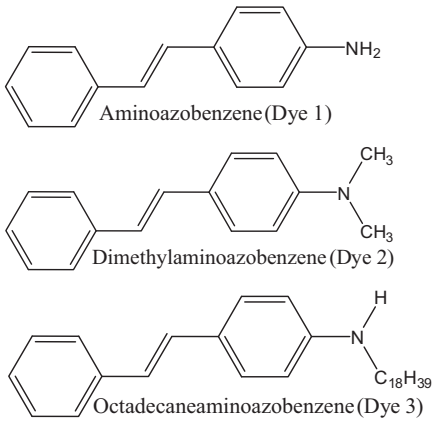

Figure 1 Structures of aminoazobenzene dyes.

less marked dependence on the nature of the embedding medium. When performing calculations to be compared with experimental results such as UV spectra, it is also important to consider the solvation effects.

Predicting the effect of a solvent on absorption spectra is a difficult task as, in principle, it requires consideration of both a fast, electronic and a slow, orientational relaxation response of a solvent [27]. Solvent effects were undertaken using four solvation models (PCM, I-PCM, SCI-PCM and IEF-PCM). λ_{max} values of three aminoazobenzene dyes were calculated using four solvation models in three solvents (cyclohexane, acetone and DMSO). Theoretical and experimental λ_{max} values are given in Table 1. Four solvation models produced similar results. Cluster analysis was also performed to display and discriminate the results of four models. Cluster analysis plot for λ_{max} calculated using four models is given in Fig. 2. Distance in figure indicates the dissimilarities between clusters. Larger the distance between two clusters, greater will be dissimilarity. Distance can be measured in a variety of ways. There are distances that are Euclidean (can be measured with a 'ruler') and there are other distances based on similarity. The squared Euclidean distance is the most used one.

Clusters of four models joined near to the distance of 3. Figure demonstrates the similarity of λ_{max} values calculated using four models. Error in the estimation of λ_{max} was also calculated by the difference of experimental and theoretical values. Error is plotted in Fig. 3. Error was found in the range of 20–70 nm. Figure clearly shows the similar trend of error. From Table 1, it is clear that a solvation model providing good results for one dye, shows poor result for the other dye.

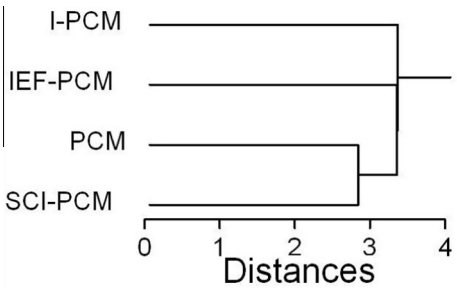

Figure 2 Dendrogram of the cluster analysis of λ_{max} calculated using four solvation models.

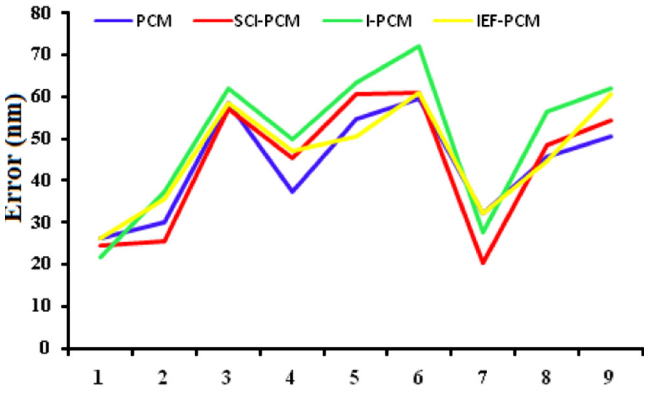

Figure 3 Error plot of λ_{max} of dyes calculated using four solvation methods (TD-DFT/BHandHLYP/6-311(d,p).

Overlapping lines in Fig. 3, conform this trend. To further elucidate the effect of basis set and functional for the prediction of λ_{max} only one solvation model (SCI-PCM) and one solvent (DMSO) was selected. This selection was made to reduce the computational cost. This selection was also facilitated to study the effect of many basis sets.

4.2. Effect of functional

Functional effect on the λ_{max} was studied using four functionals (CAM-B3LYP, LC-BLYP, BHandHLYP and PBE0). Theoretical and experimental λ_{max} values are given in Table 2. Dendrogram of cluster analysis is given in Fig. 4. Clusters of LC-BLYP and BHandHLYP join at the distance of 3. This indicates the close similarity in λ_{max} calculated by these

Table 1 λ_{max} of aminoazobenzene dyes calculated using TD-DFT/BPE0/6-311G(d,p).

Dye	Solvent	[a]Exp.	PCM	SCI-PCM	I-PCM	IEF-PCM
Dye 1	Cyclohexane	363	336.9	338.6	341.2	336.9
	Acetone	386	356.2	360.5	348.5	350.5
	DMSO	403	344.4	345.7	341.2	344.4
Dye 2	Cyclohexane	397	359.8	351.6	347.3	349.8
	Acetone	411	356.2	350.5	347.5	360.5
	DMSO	420	360.4	359.0	348.0	359.0
Dye 3	Cyclohexane	379	346.9	358.6	351.2	346.9
	Acetone	405	359.2	356.5	348.5	360.5
	DMSO	415	364.4	360.7	353.2	354.4

[a] Experimental λ_{max} of three dyes in DMSO is 403, 420 and 415 nm, respectively.

functionals. These functionals join with CAM-B3LYP at the distance of 5.3. PBE0 functional combines to other three functionals at the distance of 8.8. This indicates that λ_{max} calculated by PBE0 is different from that calculated by three functionals. From Table 2 it is found that λ_{max} calculated by PBE0 is relatively closer to experimental λ_{max}. Error in the computation of λ_{max} was also calculated. Error for four functionals was plotted and is shown in Fig. 5. From figure it is clear that error is minimum for PBE0. This is clearly seen from the plot of the errors for the various methodological combinations, for all compounds, error was in same trend.

Table 2 λ_{max} of aminoazobenzene dyes calculated in DSMO using SCI-PCM solvation methods.

Functional	Basis set	Dye1	Dye2	Dye3
CAM-B3LYP	6-31G	329.7	349.7	336.7
	6-31+G	332.6	352.6	339.6
	6-31++G	336.3	356.3	343.3
	6-31 G(d,p)	333.5	353.5	340.5
	6-31+G(d,p)	335.3	355.3	342.3
	6-31++G(d,p)	338.5	361.5	345.5
	6-311 G	345.6	368.6	352.6
	6-311+G	349.3	372.3	356.3
	6-311++G	353.3	376.3	356.3
	6-311 G(d,p)	345.3	369.3	349.3
	6-311+G(d,p)	349.0	372.7	352.3
	6-311++G(d,p)	355.0	378.5	358.5
LC-BLYP	6-31 G	332.7	359.7	335.7
	6-31+G	335.6	362.6	338.6
	6-31++G	339.3	366.3	342.3
	6-31 G(d,p)	336.5	363.5	339.5
	6-31+G(d,p)	338.3	365.3	341.3
	6-31++G(d,p)	341.5	368.5	344.5
	6-311 G	349.6	376.6	352.6
	6-311+G	353.3	371.3	356.3
	6-311++G	357.3	375.3	362.3
	6-311 G(d,p)	350.3	368.3	355.3
	6-311+G(d,p)	353.6	371.6	358.6
	6-311++G(d,p)	359.7	384.7	364.7
BHandHLYP	6-31 G	334.7	359.7	339.7
	6-31+G	337.6	362.6	342.6
	6-31++G	341.3	366.3	346.3
	6-31 G(d,p)	338.5	363.5	343.5
	6-31+G(d,p)	340.3	365.3	345.3
	6-31++G(d,p)	343.5	368.5	348.5
	6-311 G	350.6	372.6	355.6
	6-311+G	352.3	374.3	357.3
	6-311++G	356.3	378.3	360.3
	6-311 G(d,p)	345.7	359.0	360.3
	6-311+G(d,p)	352.4	374.4	356.4
	6-311++G(d,p)	358.2	380.2	362.2
PBE0	6-31 G	336.7	358.7	340.7
	6-31+G	339.6	361.6	343.6
	6-31++G	343.3	371.3	347.3
	6-31 G(d,p)	342.5	370.5	346.5
	6-31+G(d,p)	344.3	372.3	350.3
	6-31++G(d,p)	347.5	375.5	353.5
	6-311 G	354.6	382.6	360.6
	6-311+G	365.3	389.3	371.3
	6-311++G	369.3	393.3	373.3
	6-311 G(d,p)	362.3	386.3	366.3
	6-311+G(d,p)	357.9	381.9	361.9
	6-311++G(d,p)	363.1	387.1	367.1

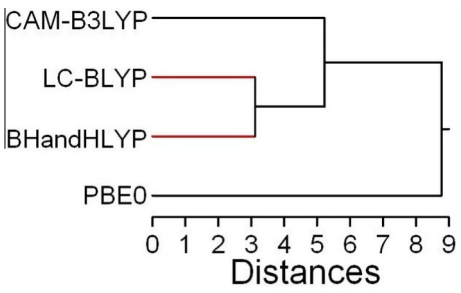

Figure 4 Dendrogram of the cluster analysis of λ_{max} calculated using four functionals.

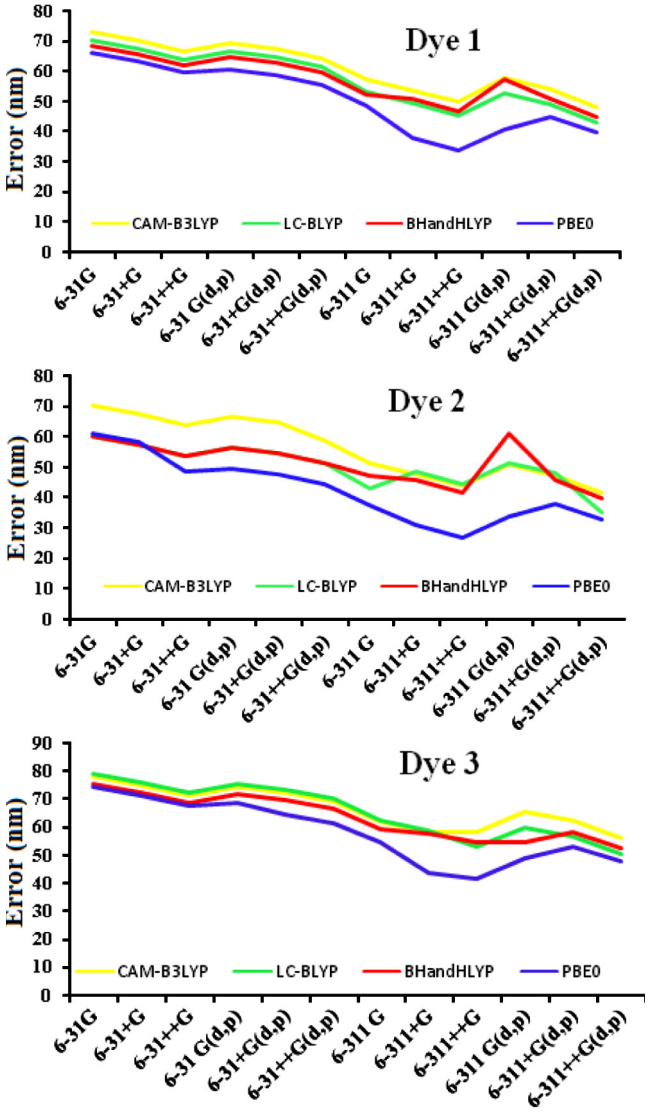

Figure 5 Error plot of λ_{max} of dyes calculated using four functionals with various basis sets.

Unlike the error plot of solvation models (Fig. 3), lines in the error plot of functionals (Fig. 5) are not overlapping.

Maximum error in the estimation of λ_{max} shown by all functionals was smaller than 80 nm. For three dyes, all functionals underestimated λ_{max}. Jacquemin et al. reported 127, 71, 12, 67, 85, and 53 nm mean signed error for HF, PBE,

PBE0, LC-PBE, LC-ωPBE, and CAM-B3LYP, respectively [28]. PBE0 yields λ_{max} in very good agreement with experimental trends. From Table 2 it is also clear that λ_{max} calculated using four functionals was red-shifted in the following order: CAM-B3LYP, LC-BLYP, BHandB3LYP, PBE0.

4.3. Effect of basis set

An ab initio calculation is strongly dependent on the number of basis functions. A small basis sets is required for the completion of calculations in short time. In this study, we have tested various basis sets. Values of λ_{max} are given in Table 2. Error in the predication λ_{max} values is also calculated. Error plots are given in Fig. 5.

Error plot shows that for three dyes error decreases up to 6-311++G basis set and then starts to increase. λ_{max} calculated by 6-311++G basis set using four functionals was closer to experimental λ_{max}. This basis set showed error in the estimation of λ_{max} between 30 and 40 nm. A further increase in the size of basis set did not show the decrease in error. So this basis set will be suitable for better accuracy and reasonable computational time. From Table 2, it is clear that the introduction of diffuse functions in the basis set red-shifted the absorbance maxima (e.g. from 6-31G to 6-31++G).

5. Conclusion

The absorption spectra of three azoaminobenzene dyes have been computed with TD-DFT approach using four solvation models, four hybrid functionals and different basis sets. All the solvation models (PCM, I-PCM, SCI-PCM and IEF-PCM) showed almost similar results. Difference between the λ_{max} calculated by four functionals was not more than 15 nm. The results of the present study point out that, although functionals provide at least satisfactory results, PBE0 is more adequate than the other functional for calculating the λ_{max} of azoaminobenzenes. The λ_{max} value always follows the PBE0 > BHandB3LYP > LC-BLYP > CAM-B3LYP sequence. For all the functionals error in estimation of λ_{max} was lower than 80 nm. In addition, it turns out that the 6-311++G basis set provided best results for all functionals: a further extension of the basis did not improve (and slightly decrease) the average quality of the theoretical prediction. This means that the absorption spectra of azoaminobenzene dyes can be accurately evaluated at a relatively small computational cost.

Acknowledgments

The authors would like to sincerely appreciate the Deanship of Scientific Research at King Saud University for its funding of this research through the Research Group Project no RGP-VPP-255.

Appendix A. Supplementary data

Supplementary data (coordinates of selected optimized dyes) associated with this article can be found, in the online version, at http://dx.doi.org/10.1016/j.jscs.2014.06.001.

References

[1] D.R. Kanis, M.A. Ratner, T.J. Marks, Design and construction of molecular assemblies with large second-order optical nonlinearities. Quantum chemical aspects, Chem. Rev. 94 (1994) 195–242.
[2] E.K.U. Gross, J.F. Dobson, M. Petersilka, Density Functional Theory, vol. 181, Springer, Berlin, 1996.
[3] M.E. Casida, C. Jamorski, K.C. Casida, D.R. Salahub, Molecular excitation energies to high-lying bound states from time-dependent density-functional response theory: characterization and correction of the time-dependent local density approximation ionization threshold, J. Chem. Phys. 108 (1998) 4439–4449.
[4] A. Dreuw, M. Head-Gordon, Single-reference ab initio methods for the calculation of excited states of large molecules, Chem. Rev. 105 (2005) 4009–4037.
[5] P.C. Chen, Y.C. Chieh, Azobenzene and stilbene: a computational study, J. Mol. Struct. (THEOCHEM) 624 (2003) 191–200.
[6] R.E. Stratmann, G.E. Scuseria, M.J. Frisch, An efficient implementation of time-dependent density-functional theory for the calculation of excitation energies of large molecules, J. Chem. Phys. 109 (1998) 8218–8224.
[7] D. Guillaumont, S. Nakamura, Calculation of the absorption wavelength of dyes using time-dependent density-functional theory (TD-DFT), Dyes Pigm. 46 (2000) 85–92.
[8] R. Improta, F. Santoro, Excited-state behavior of trans and cis isomers of stilbene and stiff stilbene: a TD-DFT study, J. Phys. Chem. A 109 (2005) 10058–10067.
[9] M. Belletete, J-F. Morin, M. Leclerc, G. Durocher, A theoretical, spectroscopic, and photophysical study of 2,7-carbazolenevinylene-based conjugated derivatives, J. Phys. Chem. A 109 (2005) 6953–6959.
[10] E.A. Badaeva, T.V. Timofeeva, A. Masunov, S. Tretiak, Role of donor−acceptor strengths and separation on the two-photon absorption response of cytotoxic dyes: a TD-DFT Study, J. Phys. Chem. A 109 (2005) 7276–7284.
[11] P. Hommen de Mello, B. Mennucci, J. Tomasi, A.B.F. da Silva, The effects of solvation in the theoretical spectra of cationic dyes, Theor. Chem. Acc. 113 (2005) 274–280.
[12] C.S. Hartley, Excited-state behavior of ortho-phenylenes, J. Org. Chem. 76 (2011) 9188–9191.
[13] D. Jacquemin, X. Assfeld, J. Preat, E.A. Perpéte, Comparison of theoretical approaches for predicting the UV/Vis spectra of anthraquinones, Mol. Phys. 105 (2007) 325–331.
[14] D. Jacquemin, E.A. Perpete, G.E. Scuseria, I. Ciofini, C. Adamo, TD-DFT performance for the visible absorption spectra of organic dyes: conventional versus long-range hybrids, J. Chem. Theor. Comput. 4 (2008) 123–135.
[15] D. Jacquemin, V. Wathelet, E.A. Perpete, C. Adamo, Extensive TD-DFT benchmark: singlet-excited states of organic molecules, J. Chem. Theor. Comput. 5 (2009) 2420–2435.
[16] D. Jacquemin, E.A. Perpete, I. Ciofini, C. Adamo, Assessment of functionals for TD-DFT calculations of singlet-triplet transitions, J. Chem. Theor. Comput. 6 (2010) 1532–1537.
[17] G.A. Shallangwa, A. Uzairu, V.O. Ajibola, H. Abba, MNDO and DFT computational study on the mechanism of the oxidation of 1,2-diphenylhydrazine by iodine, ISRN Phys. Chem. (2014) 1–8.
[18] G. Markopoulos, J. Grunenberg, Predicting kinetically unstable C═C bonds from the ground-state properties of a molecule, Angew. Chem. Int. Ed. 52 (2013) 10648–10661.
[19] D. Samanta, A. Rana, M. Schmittel, Quantification of nonstatistical dynamics in an intramolecular diels–alder cyclization without trajectory computation, J. Org. Chem. 79 (2014) 2368–2376.

[20] B. Štefane, A. Perdih, A. Pevec, T. Šolmajer, M. Kočevar, The participation of 2*h*-pyran-2-ones in [4 + 2] cycloadditions: an experimental and computational study, Eur. J. Org. Chem. (2010) 5870–5883.
[21] A. Schafer, Modern Methods and Algorithms of Quantum Chemistry, second ed., vol. 3 of NIC Johnvon Neumann Institute for Computing, Julich, 2000.
[22] M.S. Zakerhamidi, A. Ghanadzadeh, M. Moghadam, Solvent effects on the UV/visible absorption spectra of some aminoazobenzene dye, Chem. Sci. Trans. 1 (2012) 1–8.
[23] S.A. Siddiqui, T. Rasheed, M. Faisal, A.K. Pandey, S.B. Khan, Electronic structure, nonlinear optical properties, and vibrational analysis of gemifloxacin by density functional theory, Spectrosc. Int. J. 27 (2012) 185–206.
[24] S.A. Siddiqui, T. Rasheed, Quantum chemical study of IrFn (n = 1–7) clusters: an investigation of superhalogen properties, Int. J. Quantum Chem. 113 (2013) 959–965.
[25] S.A. Siddiqui, N. Bouarissa, T. Rasheed, M.S. Al-Assiri, Quantum chemical study of the interaction of elemental Hg with small neutral, anionic and cationic Au_n(n = 1–6) clusters, Mater. Res. Bull. 48 (2013) 995–1002.
[26] M.J. Frisch, et al. Gaussian 09, Revision A.1. Gaussian Inc, Wallingford, CT, 2009.
[27] A. Klamt, V. Jonas, T. Berger, J.C.W. Lohrenz, Refinement and parametrization of COSMO-RS, Phys. Chem. A 102 (1998) 5074–5085.
[28] E.A. Perpete, V. Wathelet, J. Preat, C. Lambert, D. Jacquemin, Toward a theoretical quantitative estimation of the λ_{max} of anthraquinones-based dyes, J. Chem. Theory Comput. 2 (2006) 434–440.